AD-A203 610

1/19/89
Di logged in

DTIC FILE COPY

431c042

④

Final Technical Report
on
A STUDY OF FERROELECTRICITY IN SINGLE CRYSTAL
COMPOUNDS OF THE TYPE ABF_5 AND $A_3B_2F_{12}$

ONR: *N00014-*~~87-K-0124~~87-K-0124

CMR-88-12

for the period
January 1, 1987 through June 30, 1988

DTIC
ELECTE
JAN 2 7 1989
S D
C&H

CENTER FOR MATERIALS RESEARCH

STANFORD UNIVERSITY • STANFORD, CALIFORNIA

89 ~~TDOC~~ 025 ~~88 10 18 048~~

(4)

Final Technical Report
on
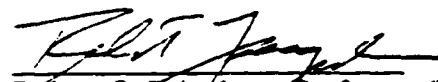# A STUDY OF FERROELECTRICITY IN SINGLE CRYSTAL COMPOUNDS OF THE TYPE ABF₅ AND A₃B₂F₁₂

ONR: *N00014-* 87-K-0124

CMR-88-12

for the period
January 1, 1987 through June 30, 1988

submitted to
the Office of Naval Research

Principal Investigator:

Robert S. Feigelson, Professor (Res.)
Center for Materials Research
Stanford, California 94305-4045
(415) 723-4007

October 1988

DTIC
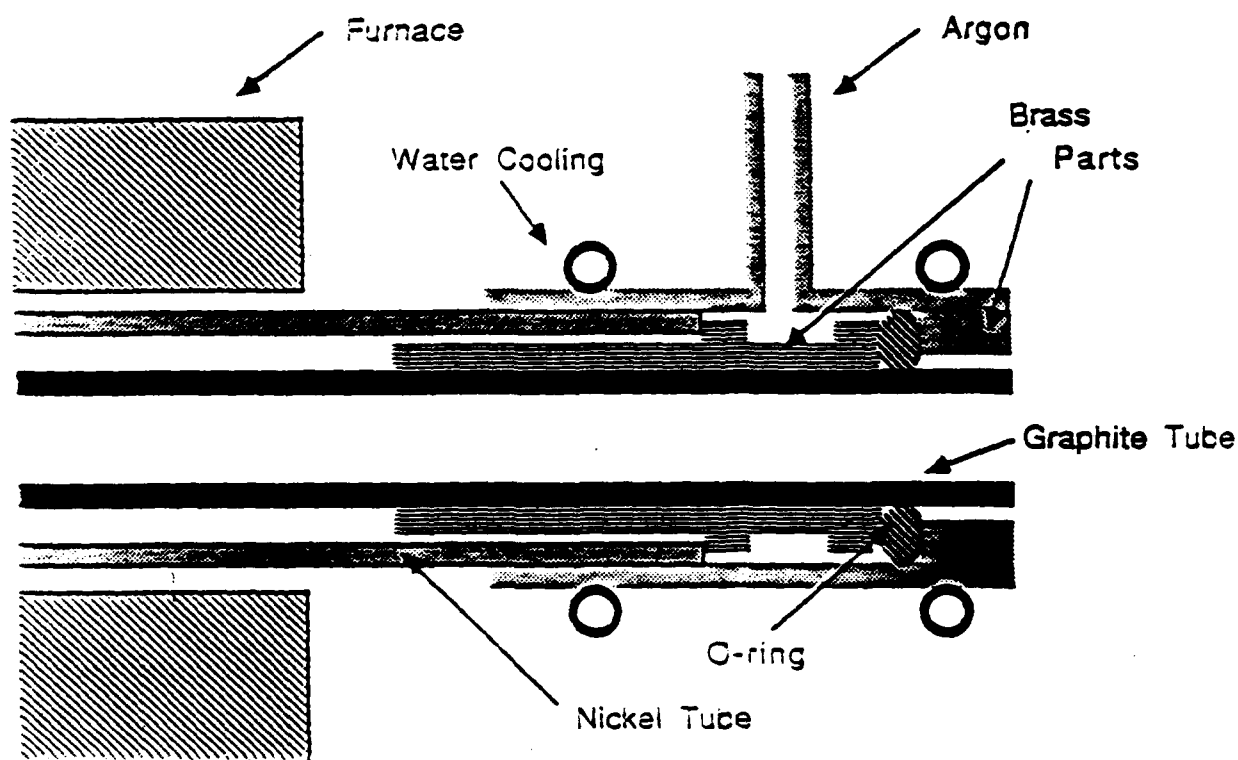ELECTE
JAN 2 7 1989
S
a
H
D

TABLE OF CONTENTS

ABSTRACT

Fig. 1 Schematic diagram of one end of HF synthesis furnace
containing a graphite reaction tube between which flows
Ti purified argon through a brass spacer. HF and/or argon
is used inside the graphite tube during synthesis or
annealing experiments.

A STUDY OF FERROELECTRICITY IN SINGLE CRYSTAL COMPOUND OF THE TYPE ABF_5 AND $A_3B_2F_{12}$

Abstract

Phase relations in the PbF_2/AlF_3 binary system were studied in order to facilitate the preparation of single crystals of a reportedly high dielectric constant ternary ferroelectric phase. A phase diagram for the composition range 50 to 100 mole percent lead fluoride was developed and crystals of the incongruently melting $Pb_3Al_2F_{12}$ phase were grown using Bridgman growth techniques. A new inverted Bridgman method was developed to help induce melt convection during growth, thereby reducing the build-up of unwanted species at the growth interface. *Lead Fluorides* *Aluminium Fluoride*

I. Introduction

The PbF_2/AlF_3 binary system contains at least two features of scientific interest: an intermediate compound with a reported peak dielectric constant of 4800 at 585 ± 10 K[1] and a lead fluoride solid solution extending to 88 mole percent PbF_2 which is reported to be an ionic conductor[2]. In our study the primary emphasis was on acquiring sufficient knowledge of the phase relations to grow single crystal samples of the intermediate compound and using them to study the dielectric anomaly.

Our goal in studying this compound was to consider its suitability as a near-millimeter range electronic phase shifter. For this application, better materials have a higher figure of merit R given by:

$$R = n^3 r$$

where n is the microwave refractive index and r is the microwave electroptic coefficient[3]. Crystals with high values of the low frequency dielectric constant and low loss tend to have high values of linear susceptibility which, in turn, indicates a large electroptic coefficient r[3,4,5]. Thus we wished to determine whether the intermediate lead aluminum fluoride compound has a high dielectric constant, low loss and a high index of refraction.

Two classes of ferroelectric fluorides are relevant to our study. These are metal fluorides with the formulae ABF_5 and $A_3B_2F_{12}$ where A is a metal of valence ± 2 and B is a metal of valence ± 3. The structure and atomic displacements during the dielectric transition have been

studied and compared for both classes[6,7,8]. Of these compounds, we chose to pursue one in the PbF_2/AlF_3 binary system because of its reported very large dielectric constant.

Phase relations in the PbF_2/AlF_3 system were previously explored by three groups: Ravez and Dumora[9], Shore and Wanklyn[10] and Joshi and Liang[2]. Ravez and Dumora[9] annealed samples of various compositions and obtained x-ray diffraction patterns for three compounds: $Pb_9Al_2F_{24}$, $PbAlF_5$ and $PbAl_2F_8$. They also found a lead fluoride solid solution from approximately 90 to 100 mole % PbF_2. Shore and Wanklyn[10] used differential thermal analysis to generate a phase diagram, x-ray diffraction of rapidly fused samples to locate the phase fields, and flux growth to obtain crystals of the central phase, which they claimed was $Pb_3Al_2F_{12}$. Ravez and Dumora[9] noted that the diffraction pattern reported by Shore and Wanklyn[10] for $Pb_3Al_2F_{12}$ was the same as that which they found for $PbAlF_5$. Aside from the $Pb_3Al_2F_{12}$ compound, the only other phase they found was a lead fluoride solid solution from 85 to 100 mole % PbF_2. Joshi and Liang[2] concentrated on studying the lead fluoride solid solution. They melted samples of varied compositions and quenched them to room temperature or annealed them for 20 hours at $400°C$. They showed that the solid solution extended to approximately 88 mole % PbF_2 by room temperature lattice parameter and conductivity measurements.

Based on this previous work, our study was directed at first identifying the stoichiometry of the central compound and clarifying the melting behavior of this compound and then growing crystals of the compound in question.

II.   Experimental Methods

For both phase equilibria studies and crystal growth experiments, either Johnson Matthey or Cerac 99.5% anhydrous aluminum fluoride powder and either Johnson Matthey Puratronic 99.997 % or Cerac precipitated, oxide-free 99.9% lead fluoride were combined and reacted in the appropriate stoichiometry. Care is necessary when working with metal fluorides to avoid moisture contamination during handling and storage of the powdered starting materials. Once the aluminum fluoride (in particular) picks up moisture from the air, it tenaciously holds water as the material is heated until oxyfluoride compounds are formed with the evolution of hydrogen fluoride gas[11]. To ensure that the intermediate compounds studied were fluorides, rather than oxyfluorides, the containers holding the starting materials were opened, stored and handled in a Vacuum Atmospheres Corporation glove box fed by nitrogen. The mixed starting materials were also reacted at elevated temperatures under a flowing hydrogen fluoride atmosphere inside a graphite tube. An o-ring sealed nickel tube surrounded the graphite, as shown in fig. 1. Argon flowing

between the nickel and graphite protected the graphite from oxygen attack when hot. Either hydrogen fluoride or dried argon was passed though the inside of the graphite tube to eliminate oxygen or water contamination. The argon was dried first by passing it through a titanium furnace.

The fluoride samples were contained in graphite containers or vitreous carbon boats during melting and heat treatment. When kept at elevated temperatures under dried argon, the fluoride samples were sometimes found, by microscopic and energy dispersive (EDS) analysis, to contain tiny metallic droplets of lead at the surface. Lead forms low temperature eutectics with platinum and gold, so the fluoride mixtures, if they contain lead, will attack and stick to containers made from these metals. The graphite and vitreous carbon containers, on the other hand, are not affected by the presence of metallic lead and the fluoride samples slid out of them easily, allowing analysis of intact samples. This was important since the melted samples generally displayed a vertical compositional gradient and examination of only a portion of the samples would lead to erroneous results.

Annealed pellets were used to determine the limits of the condensed phase regions. Aluminum fluoride and lead fluoride powders were combined to produce compositions between 33 to 100 mole % PbF_2. These powders were then loaded into covered graphite containers inside the glove box, reacted together at $730°C$ under HF, ground in a mortar and pestle inside the glove box, and then pressed into pellets in an evacuable hardened steel die. The pellets were annealed for 24 hours under dried argon at $530°C$ for compositions with greater than 60 mole % PbF_2, or $630°C$ otherwise. They were then crushed and reannealed. The samples were heated to the annealing temperature under HF in each step to minimize the contamination of the powders during heating. After processing, the pellets were examined by powder x-ray diffraction analysis using a Norelco diffractometer and also with scanning electron microscopy (SEM) and EDS.

Differential thermal analysis was used to study the melting behavior of compositions from 50 to 100 mole % PbF_2. For these experiments, PbF_2 and AlF_3 powders were combined and loaded inside the glove box into small covered graphite containers which were machined to fit onto the test thermocouples in a Dupont 1090 Thermal Analyzer. The mixed powders were first heated (using a 4 hour ramp from 530 to $730°C$) in the covered graphite containers under HF in the furnace described above. After cooling, the containers were transferred to the DTA. Heating curves for the melted fluoride mixtures were obtained under flowing dried argon at a heating rate of $10°C/minute$.

4

To study the solidus and other transition temperatures, the mixed starting materials were annealed instead of melted before being studied in the DTA. They were loaded into covered graphite cells, annealed for 24 hours at 530 or 630°C, crushed and mixed, and then loaded into the covered graphite DTA cells and reannealed. While the annealing was done under argon, the samples were heated to the annealing temperature under HF. Once again the DTA heating curves were obtained at rates of 10°C/minute. The DTA samples were examined by SEM, EDS and powder x-ray diffraction analysis to determine their phase content after heat treatment.

For the crystal growth experiments, the starting materials were melted together at temperatures ranging from 730 to 850°C under HF, then placed into a graphite crucible which is suspended inside a vertical Bridgman furnace, as shown in fig. 2. The crucible was lowered at rates between 0.5 and 1.0 mm/hour in flowing dried argon. Furnace temperature gradients of 20 to 40°C/cm at the growth interface were used in these experiments. The starting compositions used were between 50 and 73 mole % PbF_2.

The composition in various parts of the boules produced were analyzed using SEM, EDS and x-ray powder diffraction analytical techniques. Optical transmission data in the UV to visible region was obtained using a Perkin-Elmer spectrophotometer. An approximate index of refraction value was obtained using a Martin Gem Analyzer, which measures the Fresnel reflectance off a polished surface using a wavelength of 940 nm. Approximate measurements of the dielectric constant of single crystal samples were made as a function of temperature in an argon atmosphere using a Tektronix Type 130 L-C Meter.

III. Results and Discussion

The phase diagram in fig. 3 records the results of the DTA and annealing experiments. The results of Shore and Wanklyn[10] and Ravez and Dumora[9] were both found to be partly right. We found that the composition of the central phase was $Pb_3Al_2F_{12}$, that it melts incongruently at 665 ± 10°C and forms a eutectic at 565 ± 10°C with the lead fluoride solid solution, as reported by Shore and Wanklyn[10]. We also found that there is a $Pb_9Al_2F_{24}$ phase as reported by Ravez and Dumora[9] which undergoes a peritectoid transition at 555 ± 10°C, roughly 10 degrees under the eutectic melting temperature.

No evidence was found for the existence of the $PbAlF_5$ or $PbAl_2F_8$ phases reported by Ravez and Dumora[9]. Melted and annealed samples of the 33.3 and 50 mole % PbF_2 composition contained $Pb_3Al_2F_{12}$ and aluminum fluoride as determined by optical and electron
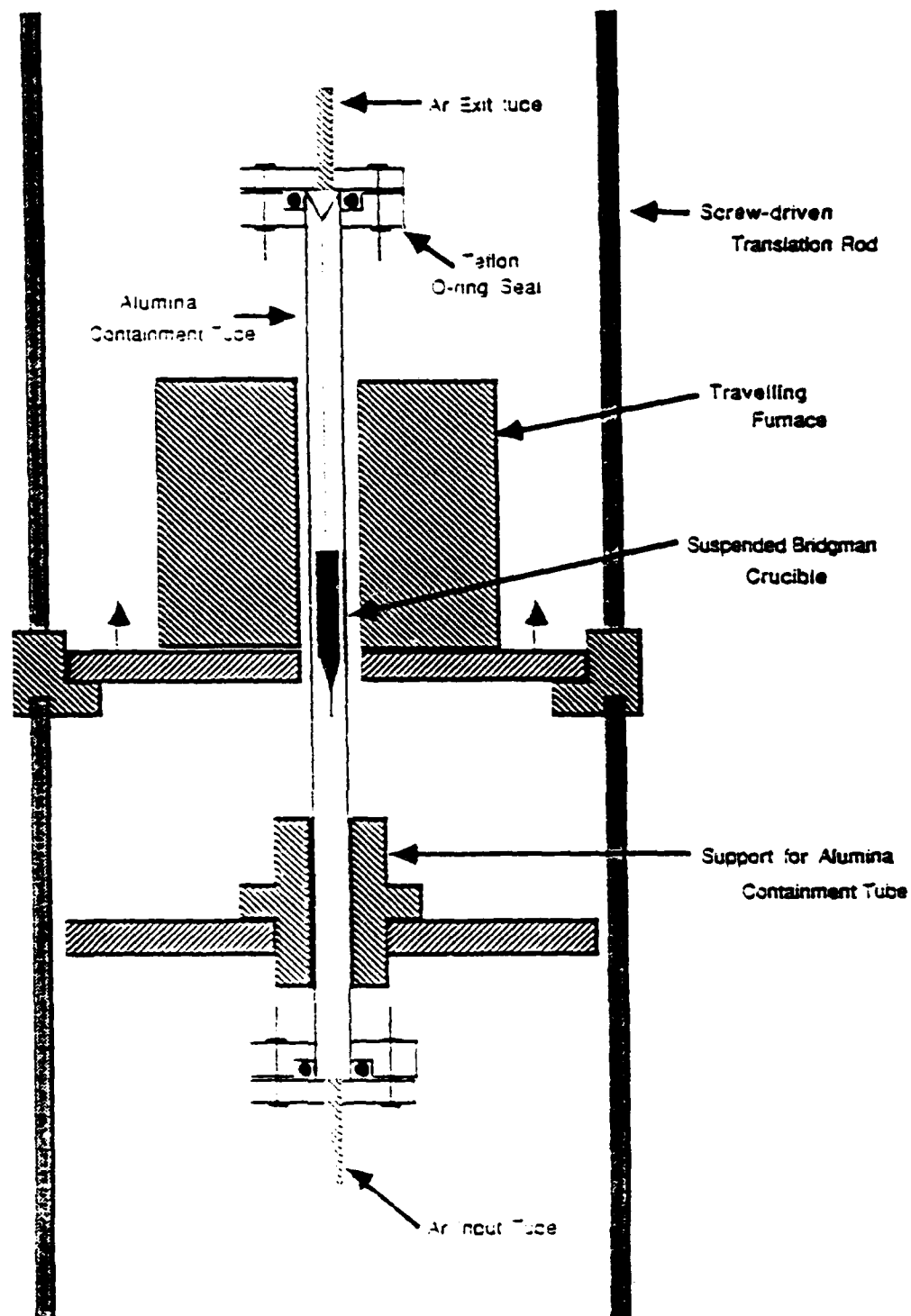
5

Fig. 2   Schematic of vertical Bridgman configuration used for both
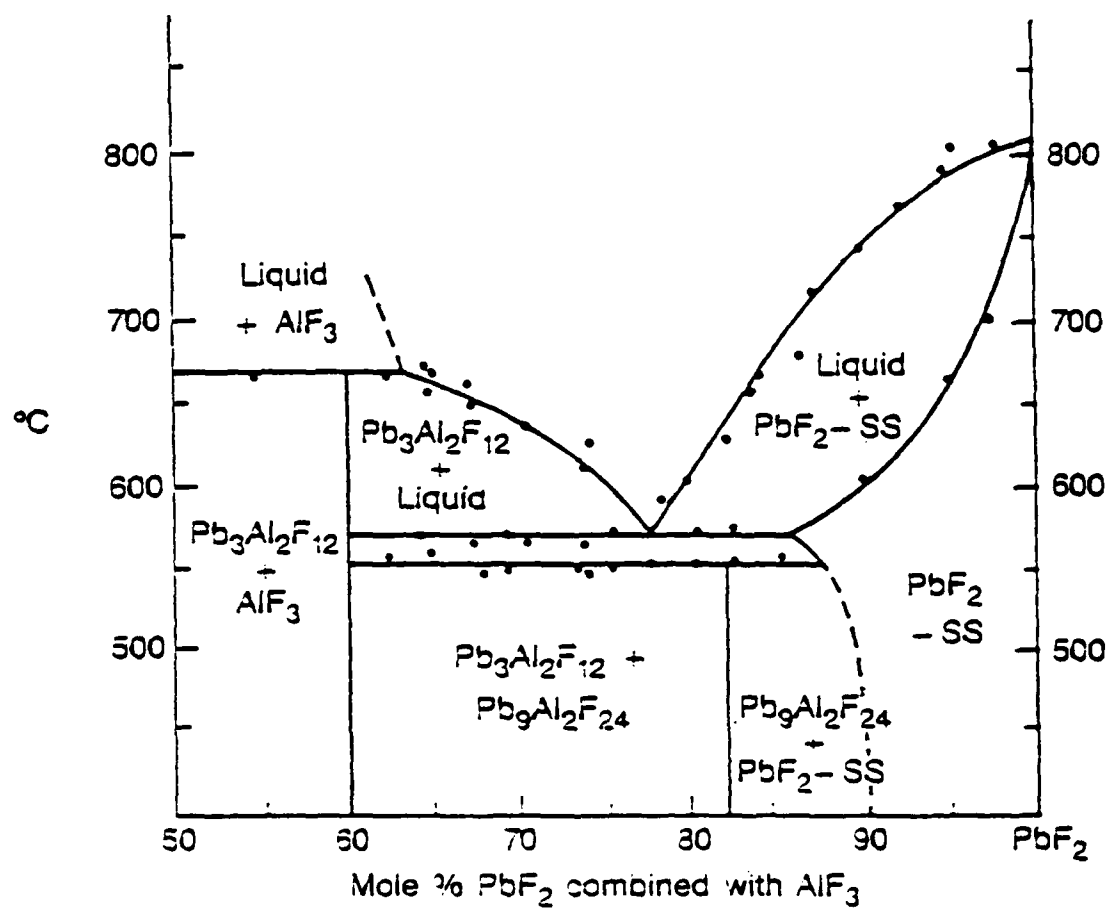standard and inverted vertical Bridgman growth.

Fig. 3   Phase field found in PbF2/AlF3 system.

microscopy. This result was confirmed by EDS analysis. However, x-ray powder diffraction patterns of samples containing 50 mole % PbF_2 by did not reveal the 16.7 mole % aluminum fluoride predicted by our phase diagram, probably due to the similarity in AlF_3 and $Pb_3Al_2F_{12}$ diffraction peaks and the greater scattering power of the $Pb_3Al_2F_{12}$ phase.

Despite vigorous efforts to observe the melting behavior of samples containing 50 to 65 mole % lead fluoride, no liquidus points were found in this temperature/composition region up to 650°. A 60 mole % PbF_2 sample was observed optically as it was heated in a platinum crucible under flowing dried argon. A slush of solid particles in a transparent liquid persisted up to $750°C$, where the vapor coming off the melt obscured the view through the furnace window. The melted sample was cut and polished. SEM and EDS examination showed the unmelted particles to be aluminum fluoride. Combining these results with the known portions of the phase diagram and melting behavior of single phase samples, it can be concluded that, while no liquidus curve can be added to the phase diagram, it would appear that $Pb_3Al_2F_{12}$ melts incongruently at $665\pm10°C$ to form liquid and aluminum fluoride and that complete melting of the 60 mole % PbF_2 composition does not occur for at least 100 degrees above that.

Based on our studies of the melting behavior of $Pb_3Al_2F_{12}$, one should be able to solidify $Pb_3Al_2F_{12}$ from a PbF_2-rich flux of composition 65 to 75 mole % PbF_2. As solidification occurs, lead fluoride will be rejected into the melt making it richer in PbF_2 until the eutectic composition is reached and eutectic solidification occurs. In practice, we found that, of the melt compositions tried between 50 and 73 mole % PbF_2, the best results obtained from vertical Bridgman growth runs were with 60 mole % PbF_2 melts. The more lead fluoride-rich melts showed earlier breakdown of the growth interface resulting in the eutectic inclusions in otherwise clear $Pb_3Al_2F_{12}$ grains shown in fig. 4.

Figures 5a and b illustrate the expected and observed phase distributions for the 60 mole % PbF_2 composition grown by the vertical Bridgman method. Solidification proceeds from the bottom, so one would expect from the phase diagram in fig. 3 that aluminum fluoride would solidify first at the bottom of the crucible, followed by $Pb_3Al_2F_{12}$ in the middle and eutectic solidification of the remaining melt near the top of the boule as shown in fig. 5a. However, instead of this order, AlF_3 was observed at the top, eutectic in the middle and $Pb_3Al_2F_{12}$ single phase material at the bottom, as shown in fig. 5b.

It was theorized that the above behavior resulted from vertical segregation of phases of differing density, producing a significant compositional gradient with height in the melt column.

Fig. 4   Eutectic inclusions in otherwise clear $Pb_3Al_2F_{12}$ gains.

Standard Vertical Bridgman Growth

Eutectic →

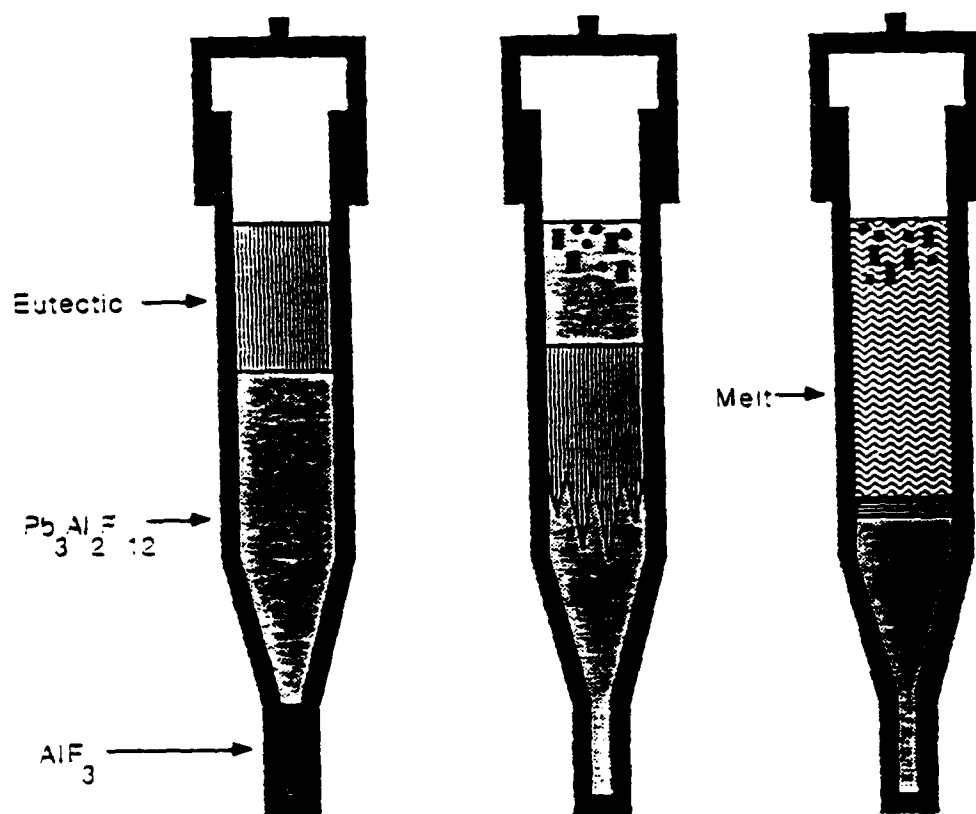Melt →

$Pb_3Al_2F_{12}$ →

AlF_3 →

Fig. 5   a) Expected phase distribution of solidified 60 mole %
PbF_2 change from phase diagram assuming complete
reaction and mixing.

b) Actual phase distribution after solidification.

c) Proposed phase distribution during growth showing
AlF_3 grains at top and PhF_2 melt enrichment layer above
growth surface.

Aluminum fluoride grains would have the lowest density and could float to the top of the melt as their solidifies or, alternatively, they could float to the melt surface before growth and remain undissolved. Thus the melt at the top would be in contact with aluminum fluoride solid and would have an aluminum fluoride-rich melt composition. The $Pb_3Al_2F_{12}$ crystallizing at the bottom of the melt, on the other hand, would cause lead fluoride to be rejected from the solidifying melt, creating a lead fluoride-enriched melt layer ahead of the growth interface. These circumstances are depicted in fig. 5c which shows a diagram of a 60 mole % PbF_2 charge during a growth run. This scenario is supported by the distribution of phases found in our Bridgman boules and the occurrence of cellular breakdown to the eutectic rod inclusions in all of our standard Bridgman runs. Diffusion and convection in the melt could counter the buildup of such a compositional gradient, but the lead fluoride-rich melt at the bottom would be denser, rendering solutal convection unlikely and the cold zone is at the bottom, so thermal convection should not be pronounced.

In order to test the above suppositions, inverted vertical Bridgman growths of the 60 and 65 mole % PbF_2 compositions were tried. The charge was loaded into a standard crucible, then raised rather than lowered through the furnace. The charge thus is solidified downward, the top of the melt solidifying first. While this technique has some disadvantages which will be discussed later, it encourages natural convection (mixing) and therefore discourages the formation of a compositional gradient in the melt. The aluminum fluoride grains which form first and are lighter than the melt would not migrate in the inverted density gradient and the lead fluoride which is rejected during the solidification of $Pb_3Al_2F_{12}$ and is heavier than the melt will be transported down by solutal convection. Mixing by thermal convection would also be encouraged since the hotter, less dense melt is at the bottom. Figure 6 summarizes the expected results and those obtained, along with the expected phase distribution during solidification.

For inverted Bridgman growth runs, the experimental results were in good agreement with those predicted. The aluminum fluoride in the 60 mole % lead fluoride growth run was segregated at the top of the boule, the middle region held single phase $Pb_3Al_2F_{12}$ and at the bottom there was a flat interface between the $Pb_3Al_2F_{12}$ grains and the eutectic, rather than breakdown to eutectic rod inclusions. The 65 mole % lead fluoride run, on the other hand, showed no aluminum fluoride at the top, just $Pb_3Al_2F_{12}$ grains in the upper portion and eutectic on the bottom. Figure 7 shows a clear, but cracked grain from the 60 mole % lead fluoride inverted Bridgman run and fig. 8 shows the same grain through which one can see the letters and texture of the paper behind it.
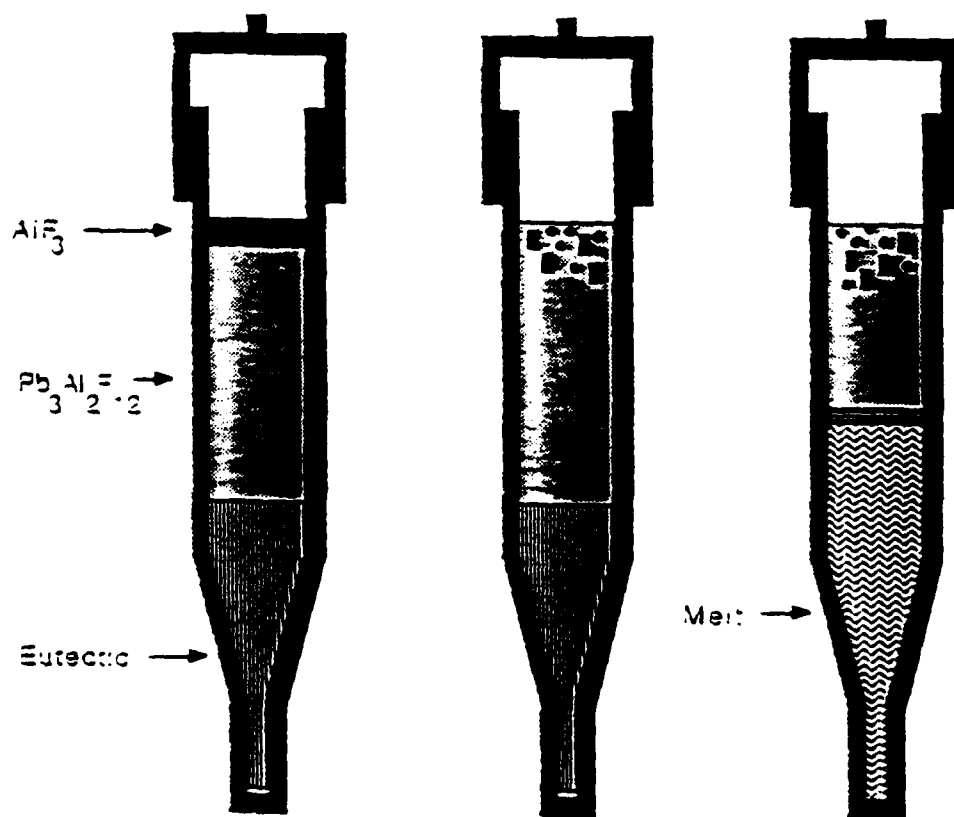
7

Inverted Vertical Bridgman Growth

Fig. 6   a) Expected phase distribution of solidified 60 mole %
PbF$_2$ charge from phase diagram assuming complete
reaction and mixing.

b) Actual phase distribution after solidification.

c) Proposed phase distribution during growth.

Fig. 7   Micrograph of $Pb_3Al_2F_{12}$ grain in transmitted light from 50 mole % PbF_2 inverted vertical Bridgman growth run.
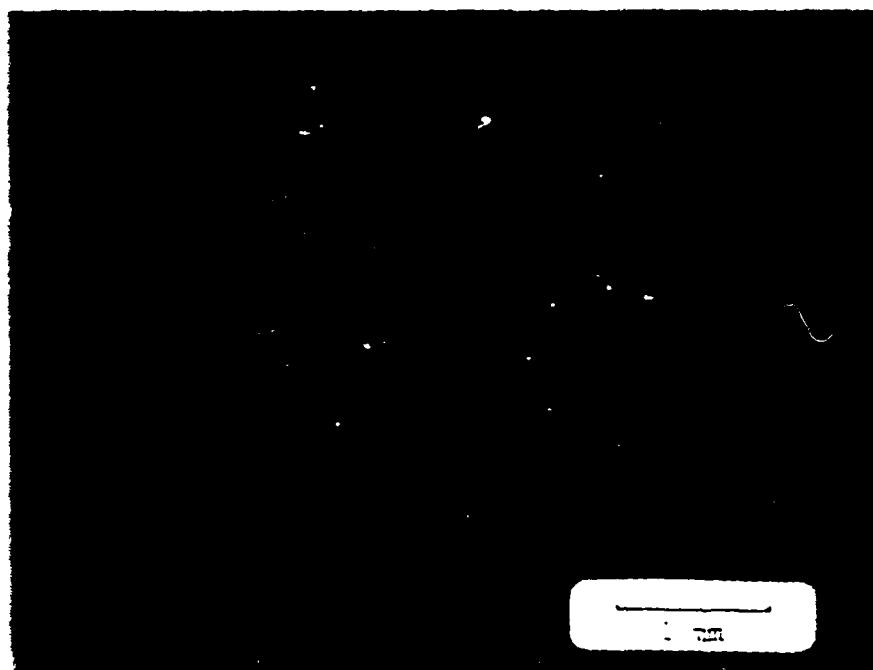
Fig. 8   Micrograph of grain in fig. 7 backed by lettering printed on paper.

The inverted vertical Bridgman growth runs produced a larger relative fraction of inclusion-free $Pb_3Al_2F_{12}$ solid grains, but these grains were smaller in size than those produced by standard vertical Bridgman growth, had a different crystallographic orientation, and showed more severe cracking. Because the volume of the melt is greater than the volume of the solid, as the melt solidifies from the top a shrinkage hole in the center of the $Pb_3Al_2F_{12}$ boule develops. In cross sections of boules, 5 to 8 grains predominated because grain selection is not effective without a seed or a capillary. Since the boule was hollow, no central grain developed and the outside grains had less chance to grow larger. The orientation of these grains differed from that which was seen before suggesting that the initial grains which nucleated did not grow parallel to the axis of the growth crucible.

Figure 9 shows the isogyre pattern of the polished cross-section of a grain from a standard vertical Bridgman growth run and indicates that this grain grew with its c-axis very near to the boule axis (normal to the polished face). Such an isogyre pattern typifies that seen for the central grain in the standard vertical Bridgman growth runs. The cross in the isogyre pattern could also be seen in the other grains of standard growth runs by tilting the polished cross-section. While polished sections from the inverted vertical Bridgman growths show extinction under crossed polarizers, the central cross indicating the c-axis orientation was not visible, even with tilted samples. Thus, the c-axis appears to be oriented at large angles from the boule axis. This change in grain orientation from the standard Bridgman runs could cause stresses in the crystals due to asymmetric thermal contraction during cooling, causing the increased cracking, especially at the grain boundaries, observed in the inverted Bridgman boules.

Transparent $Pb_3Al_2F_{12}$ grains from both the standard and inverted vertical Bridgman growth runs were used to make physical property measurements. Density measurements were made on a grain from a 60 mole % lead fluoride standard run, using Avogadro's principle, i.e. finding the sample volume by its fluid displacement. Kerosene was used in these experiments. A value of 6.64 gm/cc was measured which compares well with Shore and Wanklyn's[10] experimental value of 6.47 for the $Pb_3Al_2F_{12}$ phase. Our value may be off somewhat due to the rough sample surfaces, but it is much closer to [10] than to the $PbAlF_5$ phase of Ravez and Dumora[9] who's values of 5.956 (calculated) and 5.91 (experimental) are very low by comparison.

Optical and infrared absorption measurements were made on a clear sample of $Pb_3Al_2F_{12}$ grown from a 60 mole % lead fluoride charge using the standard vertical Bridgman technique. This data is shown in the transmission vs. wavelength plot of fig. 10. The long wavelength edge

Fig. 9   Conoscropic figure taken in direction perdendicular to the
           face of a transparent $Pb_3Al_2F_{12}$ sample. Viewing direction
           is down the growth axis.
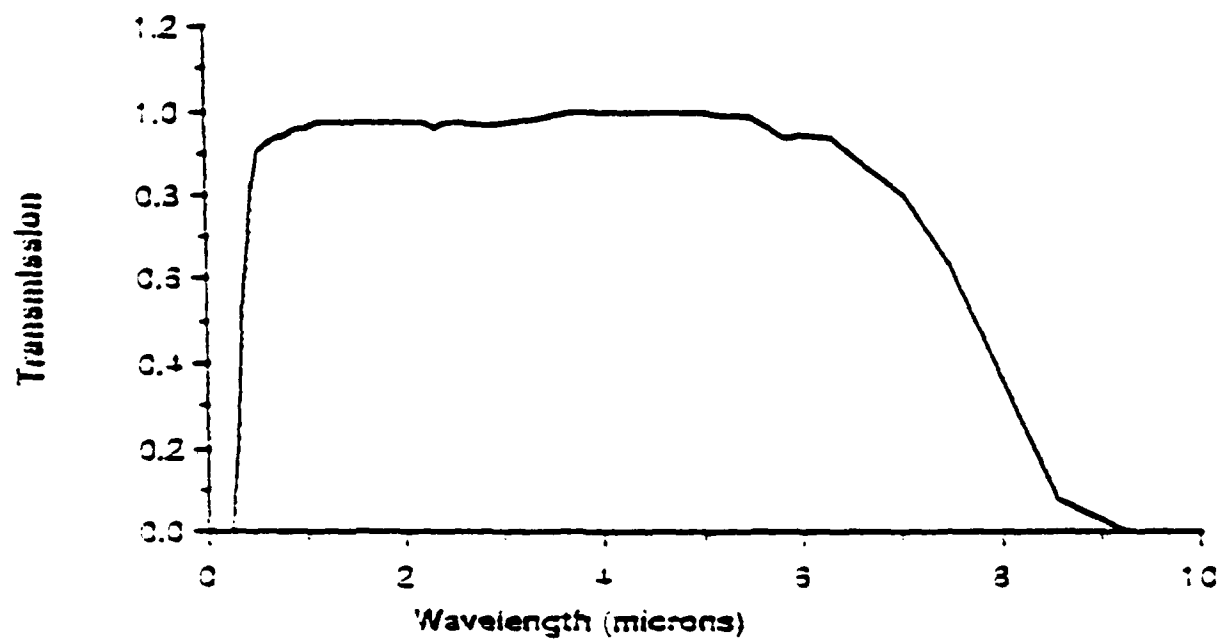
Fig. 10 Relative spectral transmittance of Pb₃Al₂F₁₂ crystal. Some small absorption peaks, probably associated with bound and absorbed H₂O, can be seen.

begins at about 6 microns and zero transmittance occurs at about 9 microns. The short wavelength edge was found to be at 0.26 microns. This broad transparency range is typical of fluoride crystals. Lead fluoride, for example, is transparent from 0.29 to 11.6 microns. Several small absorption peaks were observed near 2.7 and 6 microns and are probably due to bound water and also water adsorbed on the surface.

The index of refraction was measured to be roughly 1.6 to 1.65, depending on the sample tested.

The capacitance of flat, single crystal samples with gold or graphite contacts was determined as the sample was heated in an argon atmosphere. The dielectric constant as a function of temperature was then calculated from this data. Maximum relative dielectric permitivities found at the dielectric anomaly ranged between 70 to 150 at temperatures ranging from 480° to 530° Kelvin. The agreement between these results and those of Ravez et al. for a sintered pellet is poor. They reported[1] a peak dielectric constant of 4800 at 585°K. More extensive measurements are planned to resolve this discrepancy.

IV. Conclusions

Phase relations in the PbF_2/AlF_3 binary system were determined using DTA and annealing experiments to facilitate the preparation and examination of single crystals of a reported intermediate ferroelectric phase. A phase diagram for the composition range 50 to 100 mole percent lead fluoride was developed and crystals of the incongruently melting $Pb_3Al_2F_{12}$ phase were grown using both the standard and an inverted Bridgman growth technique. Measurements on the samples grown provided information on the optical transmittance, index of refraction, density, and dielectric behavior of $Pb_3Al_2F_{12}$. The transmission range was found to be from 0.26 to 6 microns, the index of refraction around 1.6 to 1.65 at 940 nm and the density 6.64 gm/cc. Our samples showed a dielectric anomaly with a peak relative permitivity an order of magnitude lower than that reported[1] for a sintered pellet sample, at a temperature of 480 to 530°K as opposed to the reported transition at 585°K.

V. REFERENCES

1. J. Ravez, S. C. Abrahams, J. P. Chaminade, A. Simon, J. Grannec, and P. Hagenmuller, Ferroelectrics 38, 773 (1981).

2. A. V. Joshi and C. C. Liang, J. Electrochem. Soc. 24, 1253 (1977).

3. M. B. Klein, Int. J. of Infrared and Millimeter Waves 2 ,239 (1981).

6. R. von der Muhll, S. K. Kurtz, and P. B. Jamieson, Phys. Rev. 172, 551 (1968).

7. S. C. Abrahams, J. Ravez, S. Canuouet, J. Grannec, and G. M. Loiacono, J. Appl. Phys. 55, 3056 (1984).

8. J. Ravez, R. von der Muhll and P. Hagenmuller, J. Sol. State Chem. 14, 20 (1975).

9. J. Ravez and P. Dumora, C. R. Acad. Sci. 269, 331(1969).

10. R. G. Shore and B. M. Wanklyn, J. Amer. Cer. Soc. 52, 79(1969).

11. Final Technical Report, Contract Number N00014-82-0266, June 5, 1987.

VI. COGNIZANT PERSONNEL

For supplementary information relating to this report, please contact the following:

For technical matters:

> Professor R. S. Feigelson
> Center for Materials Research
> (415) 723-4118

For administrative matters:

> M. I. Hogan
> Administrator
> Center for Materials Research
> (415) 723-0197

For financial matters:

> E. T. Winfield
> Financial Officer
> Center for Materials Research
> (415) 723-0400

For contractual matters:

> Robert Baum
> Contract Officer
> Sponsored Projects Office
> Stanford University
> (415) 723-4671